Pure & Appl. Chem., Vol.55, No.1, pp.23-34, 1983.
Printed in Great Britain.

0033-4545/83/010023-12$03.00/0
Pergamon Press Ltd.

METAL PEPTIDE COMPLEXES

Dale W. Margerum

Department of Chemistry, Purdue University, West Lafayette, Indiana 47907, USA

Abstract - Deprotonated N(peptide) and N(amide) groups are very strong donors which help to stabilize the trivalent oxidation states of copper and nickel. The Cu(III,II) potentials are highly dependent on the nature of the coordinated peptide. The lower the electrode potential the slower the redox decomposition reaction of the Cu(III)-peptide to give Cu(II) and oxidized ligand. Methyl groups in place of hydrogens on α-carbon atoms decrease the thermal decomposition, but increase the photochemical decomposition with relatively high quantum yields (Φ) in both UV and visible. The Φ values and the redox products are wavelength dependent. The copper(III) peptides are four-coordinate, square planar complexes which are slow to undergo equatorial substitution. The Cu(III,II) electron transfer reactions are rapid and are enhanced by an inner-sphere axial path. The Ni(III)-peptide complexes are six-coordinate with tetragonal distortion. Axial substitutions are very labile while equatorial substitutions are sluggish. The Ni(III,II) electron transfer reactions are rapid and are also enhanced by an inner-sphere axial path. The Ni(III) peptides will add a second peptide or other chelating agents to form stable bis-peptide or ternary complexes.

INTRODUCTION

Copper(II) and nickel(II) react readily with oligopeptides to form metal-N(peptide) bonds and release peptide hydrogen ions (Ref. 1). The value of n in eq 1 can vary from 1 to 3 for

$$M^{2+} + L \rightleftharpoons M(H_{-n}L)^{2-n} + nH^{+} \qquad (1)$$

linear peptides and is 4 for a cyclic tetrapeptide (Ref. 2) and for N-formyl tetrapeptides (Ref. 3). The pH for the first proton release varies with the metal ion and the peptide. Typical pH ranges are 2-4 for Pd(II), 3-6 for Cu(II), 7-8 for Ni(II) and 10-11 for Co(II) (Ref. 1). Stepwise proton loss occurs with Cu(II) oligopeptides, for example the pK_a values for tetraglycine (G_4) are 5.4, 6.8 and 9.1 for the formation of $Cu^{II}(H_{-1}G_4)$, $Cu^{II}(H_{-2}G_4)^{-}$ and $Cu^{II}(H_{-3}G_4)^{2-}$, respectively (Ref. 4). In recent work with peptide complexes of α-aminoisobutyric acid (Aib = $NH_2C(CH_3)_2COOH$) we found pK_a values of 4.2 and 6.1 for the formation of $Cu^{II}(H_{-1}Aib_3)$ and $Cu^{II}(H_{-2}Aib_3)^{-}$ and a first ionization pH as low as 3.5 for $Cu^{II}(H_{-1}Aib_2)$ formation (Ref. 5). The structures of a number of copper(II) and nickel(II) peptide complexes were determined in the extensive x-ray crystallographic studies of Freeman (6). This work along with solution studies firmly established that when metal ions coordinate to the peptide nitrogen the proton is displaced.

Proton transfer kinetics. The kinetics of the reverse reaction in eq 1 indicate that while protons may attack the coordinated peptide nitrogen, the simultaneous metal coordination and protonation of nitrogen is a transition state and not a stable species (Ref. 1, 7, 8). On the other hand, the peptide oxygen can be protonated to form stable species which have been isolated in crystalline form (Ref. 9) and shown by equilibrium and kinetic studies to exist in solution (Ref. 9-14). Figure 1 shows the protonation pathways. We have termed the N-peptide proton transfer mechanism an "inside" protonation because it takes place with an atom in the inner coordination sphere of the metal and we have termed the reaction at the peptide oxygen an "outside" protonation because the oxygen atom is outside the first coordination sphere of the metal. The outside protonation pathway is not general-acid catalyzed and the protonated species may be present as a major species in solution with pK_a values of 1 to 4. The inside protonation pathway is general-acid catalyzed and displays special characteristics which indicate that simultaneous metal ion solvation occurs. Thus, the

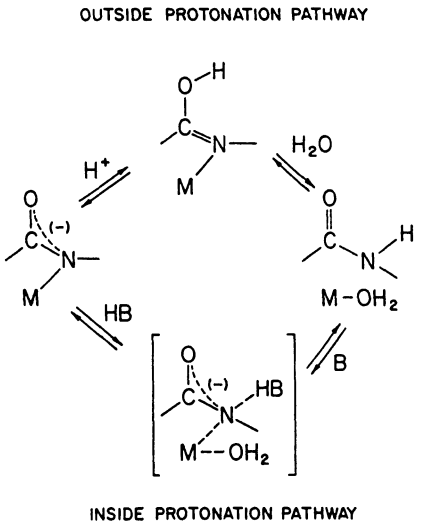

Fig. 1. Mechanism for the proton transfer reactions of metal peptide complexes.

Brønsted plots shown in Fig. 2 (Ref. 15-17) have strong curvature and reach a limiting value

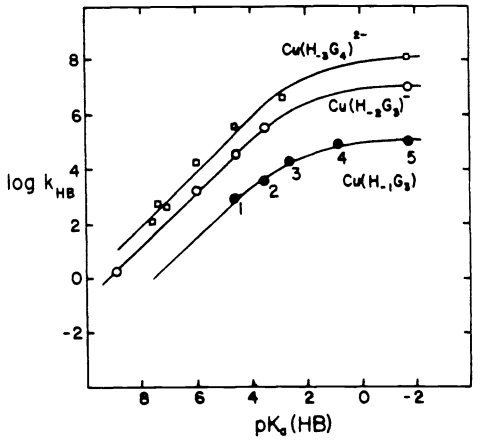

Fig. 2. Brønsted plots for reactions of HB with Cu(II) peptide complexes.

for the rate constants which are far below the diffusion limit of 10^{10} M^{-1} s^{-1}. The reactions of $Cu^{II}(H_{-1}G_3)$ show this behavior distinctly with the rate constant of 10^5 M^{-1} s^{-1} for $Cl_2CHCOOH$ (point 4) equal to the rate constant for H_3O^+ (point 5). This behavior can be explained by a modified (Ref. 18-20) Marcus theory (Ref. 21-22) of proton transfer. The modification changes the W_R value in the Marcus theory from a simple work term (required to bring the reactants together) to a larger energy term which arises from the need to solvate the metal ion as shown in Fig. 1. The three curves drawn in Fig. 2 are based on the following Marcus parameters: (kcal mol^{-1}) for $Cu(H_{-3}G_4)^{2-}$, $\lambda/4$ 1.8, W_R 6.0; for $Cu(H_{-2}G_3)^-$, $\lambda/4$ 1.6, W_R 7.7; for $Cu(H_{-1}G_3)$, $\lambda/4$ 1.1, W_R 10.4 (Ref. 17, 23). The intrinsic barrier ($\lambda/4$) is small. This accounts for the abrupt change of slope of the Brønsted plots. As the W_R term

increases the rate constants reach a plateau at lower values. The W_R values tend to increase with the strength of the metal-peptide bond. As the metal peptide bond becomes stronger and higher acid concentrations are needed to cause the reaction, contributions from the outside protonation pathway tend to become more important.

Substitution reactions. The substitution reactions of metal peptide complexes are interesting because of the variety of observed reaction paths. Two features of the metal-peptide complexes which contribute to these multiple pathways are the protonation character already discussed and the readily available axial coordination sites. Incoming multidentate ligands can obtain a coordination foothold in an axial position and often appear to also coordinate to one equatorial position prior to rate-determining step in which the metal-N(peptide) bond is broken (Ref. 1). As a result, multidentate ligands are particularly effective as nucleophiles. Pronounced steric effects are found in these nucleophilic substitution reactions. This is true for both the incoming ligand and the leaving peptide. In recent studies with triethylenetetramine displacement of copper(II) tripeptides (eq 2) the rate

$$Cu^{II}(H_{-2}L)^{-} + \text{trien} \xrightarrow{k} \text{Cutrien}^{2+} + L^{-} \qquad (2)$$

constants vary by eight orders of magnitude for G_3 (1.1×10^7 M^{-1} s^{-1}) (Ref. 24) compared to Aib_3 (1.4×10^{-1} M^{-1} s^{-1}) (Ref. 23, 25). Steric hindrance of the methyl groups in Aib_3 interfere with the equatorial coordination of trien and also decrease the rate of opening the peptide chelate ring.

There is strong evidence for combined nucleophilic and acid attack. This is observed in two ways. One is the special effectiveness of coordinating acids in protonation studies (Ref. 7). This is attributed to the axial coordination of the nucleophilic end of these acids while the acidic end takes part in a general acid catalyzed proton transfer to the peptide nitrogen. A second important behavior is a proton-assisted nucleophilic mechanism in which a proton attacks the peptide nitrogen as a nucleophile coordinates the metal (Ref. 11, 26). This is very similar to the behavior described in the general-acid catalysis where the W_R term is associated with metal ion solvation. The stronger nucleophiles permit proton transfer to the peptide nitrogen to occur more readily and this protonation in turn tends to reduce the metal coordination number making the nucleophilic attack more favorable.

Spontaneous O_2 uptake by nickel(II) and copper(II) peptides. Solutions of $Ni^{II}(H_{-3}G_4)^{2-}$ at pH 7-9 react with dissolved oxygen to give a yellow intermediate which in turn gives selectively oxidized peptides (Ref. 27). A similar reaction occurs with $Cu^{II}(H_{-3}G_4)^{2-}$, but the oxygen uptake is light inhibited (Ref. 28). In both instances a trivalent metal complex is the yellow intermediate which is observed and these $Ni^{III}(H_{-3}G_4)^{-}$ and $Cu^{III}(H_{-3}G_4)^{-}$ species activate the reactions with O_2. The detailed kinetics of these autoxidation reactions have been reported (Ref. 29, 30). It is worth noting that the spontaneous nature of these reactions led directly to our studies of the chemistry of Ni(III) peptides and Cu(III) peptides as well as their photochemical behavior.

COPPER(III) PEPTIDES

Properties of Cu(III) peptide complexes. Some of the evidence for the existence of trivalent copper in the peptide complexes has been reviewed recently (Ref. 31). In addition to O_2, oxidizing agents such as $IrCl_6^{2-}$ and $S_2O_8^{2-}$ can be used. Electrochemical oxidation in a flow-through electrolysis column is a convenient way to generate Cu(III)-peptide complexes. The resulting complexes are able to oxidize iodide ion or ascorbic acid with full recovery of the original peptide, which indicates that the metal center rather than the peptide has been oxidized. The redox reaction in eq 3 was used in competition with the acid-base

$$Ir^{IV}Cl_6^{2-} + Cu^{II}(H_{-3}G_4)^{2-} \rightleftharpoons Ir^{III}Cl_6^{3-} + Cu^{III}(H_{-3}G_4)^{-} \qquad (3)$$

reactions of $Cu^{II}(H_{-3}G_4)^{2-}$, $Cu^{II}(H_{-2}G_4)^{-}$, $Cu(H_{-1}G_4)$ and CuG_4^{+} to establish that the stoichiometry of the Cu(III) species was $Cu^{III}(H_{-3}G_4)^{-}$ and to obtain its electrode potential (Ref. 32). The Cu(III) complex does not dissociate in dilute acid, while the Cu(II) complex dissociates rapidly. The sluggish substitution reactions of the Cu(III) complex and its ability to pass through an ion exchange column which removes Cu(II) from the peptide was important initial evidence for Cu(III). The eluent had no ESR spectra, the UV-VIS spectra were completely different from that of Cu(II) peptide complexes, and the eluent had oxidizing power.

Cyclic voltammetry of Cu(II) peptides has been used to determine the Cu(III,II) electrode potentials for more than 40 complexes (Ref. 3). The E^o values range from 1.02 V for the GGhisG complex to 0.37 V for the Aib_3a complex. Some representative values are 0.92 for G_3, 0.81 for A_3, 0.66 for Aib_3, 0.63 for G_4 and 0.48 for the macrocyclic tetrapeptide, C (Ref. 14). Lower E^o values occur with an increase in the number of deprotonated-peptide or deprotonated amide groups. E^o values also decrease as alkyl groups replace hydrogens on the α-carbon atoms and E^o values are lower for 5-membered rings as opposed to 6-membered rings.

The temperature dependence of the electrode potential provides a measure of the change in entropy for the reduction: $dE^o/dt = \Delta S^o/nF$. The average ΔS^o value is -14 cal deg^{-1} mol^{-1} for six $Cu^{III,II}$ peptide couples (Ref. 33). The large negative entropy change can be accounted for by the increase in axial solvation of copper upon its reduction in accord with eq 4. Copper(II) complexes are known to be six coordinate with tetragonally distorted

$$Cu^{III}(H_{-n}L) + 2H_2O + e^- \longrightarrow Cu^{II}(H_{-n}L)(H_2O)_2 \qquad (4)$$

geometry, so the presence of two axial water molecules is expected. The results show, however, that the Cu(III) peptide complex is only four coordinate with no axial solvation.

These results predict that the E^o for the Cu(III,II) couple will decrease greatly as the activity of water is reduced. This is the case. As the solvent is changed to one with weaker coordinating properties the E^o value decreases markedly. The value for $Cu^{III,II}(H_{-2}Aib_3)$ decreases from 0.66 V in water to 0.12 V in acetonitrite.

The crystal structure of the thermally stable copper(III) peptide complex, $Cu^{III}(H_{-2}Aib_3)\cdot 2H_2O\cdot 1.5\ NaClO_4$, has been determined (Ref. 34). The Cu(III) is four coordinate with the four donor atoms coplanar within ± 0.06 Å and in a nearly square-planar geometry with bond lengths (Å) of 1.989(5) for Cu^{III}-N(amino), 1.801(4) and 1.804(5) for the two Cu^{III}-N(peptide) and 1.826(3) for Cu^{III}-O(carboxyl). These metal-ligand bonds are 0.12 to 0.17 Å shorter than the equivalent Cu(II) bonds (Ref. 6). The bond angles for the chelate rings average 87.3° for this Cu(III) peptide compared to 83° for Cu(II) peptide complexes. There appears to be no axial coordination as the closest contact distance is 2.91 Å for a perchorate oxygen.

The Ni(II) peptide complexes are also low spin d^8, square planar complexes but the Cu(III) bond distances are shorter by 0.02 and 0.04 Å for the metal-amino and metal-N(peptide) groups. The shorter Cu(III) donor bonds allow the peptide donors to form a more ideal square-planar array around copper(III) than for copper(II) or nickel(II).

In-plane substitution. Equatorial substitution reactions of Cu(III) peptides are slow with the excention of the terminal N(peptide) group. When $Cu^{III}(H_{-3}G_4)^-$ is placed in 0.1 M acid the terminally coordinated group dissociates with a rate constant of 0.3 s^{-1}. Subsequent substitution reactions are not observed prior to self-redox decomposition which varies from 3.5×10^{-5} s^{-1} in neutral solution to 0.013 s^{-1} in 0.4 M $HClO_4$ (Ref. 13). The Cu(III) complex of Aib_3a is very stable in acid solution but undergoes reversible spectra shifts in strong acid as seen in Fig. 3. The presence of 3 isobestic points indicate that there are only two main absorbing species and the data fit a protonation constant of 1.78 (pK_a 0.25). The spectral shifts are characteristic of the change from three deprotonated(N-peptide) groups to two deprotonated(N-peptide) groups observed for other Cu(III) peptide complexes. The reaction which takes place is seen in Fig. 4 where the second order rate constant for protonation is 0.02 M^{-1} s^{-1}. Once again the terminal peptide group of Cu(III) undergoes a substitution reaction, but no other substitution is observed. Even in 4 M $HClO_4$ no additional spectral shifts occur although there is a 25% loss of Cu(III) in 30 days (Ref. 35).

Amine deprotonation in base. Earlier work reported the ionization of amine protons from Cu(III)-peptide complexes at pH 11-12 (Ref. 36). The color change from yellow to red in these reactions is striking, but a stopped-flow vidicon spectrometer was needed to obtain spectra of the red species because of the rapid redox decomposition reactions in base. The $Cu^{III}(H_{-2}Aib_3)$ complex, with no hydrogens on the α-carbons, is much more stable in base and the full UV-VIS spectral shifts of the amine deprotonation reaction to give $Cu^{III}(H_{-3}Aib_3)^-$

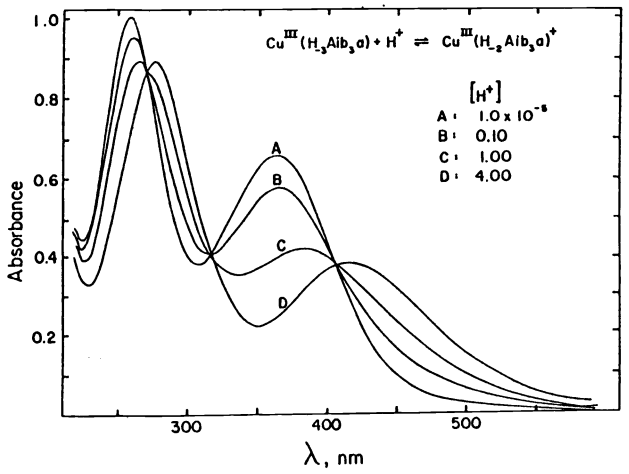

Fig. 3. Absorption spectra of the Aib_3a complex of Cu(III) in acid.

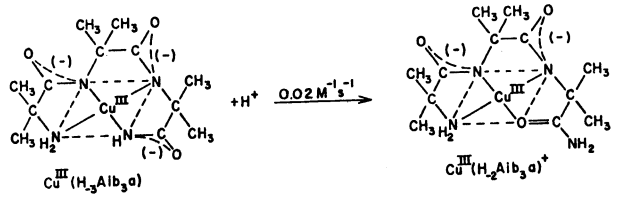

Fig. 4. Protonation of $Cu^{III}(H_{-3}Aib_3a)$ to form $Cu^{III}(H_{-2}Aib_3a)^+$.

are given in Fig. 5. The pK_a value is 11.6. There are at least three charge transfer bands at 550, 320, and 250 nm for the Cu(III)-amine deprotonated complex.

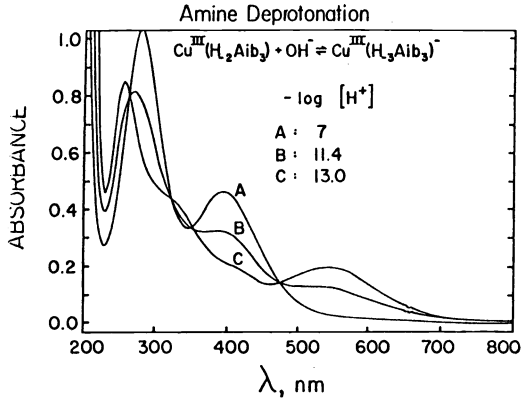

Fig. 5. Absorption spectra of $Cu^{III}(H_{-2}Aib_3)$ and its amine deprotonated product, $Cu^{III}(H_{-3}Aib_3)^-$.

Thermal redox decomposition. The redox decomposition of Cu(III)-peptides is both acid and base catalyzed. At pH 7 the $Cu^{III}(H_{-3}G_4)^-$ complex has a half life of 5.5 h and the macrocyclic tetrapeptide complex, $Cu^{III}(H_{-4}C)^-$, has a half life of 6 weeks (Ref. 14). On the other hand, both of these complexes decompose in a few minutes at pH 0 or pH 14. Figure 6 shows the log of the rate constant for redox decomposition at pH 11 plotted against E^o for Cu(III,II) couples. As the E^o increases the redox decomposition rate increases. The half

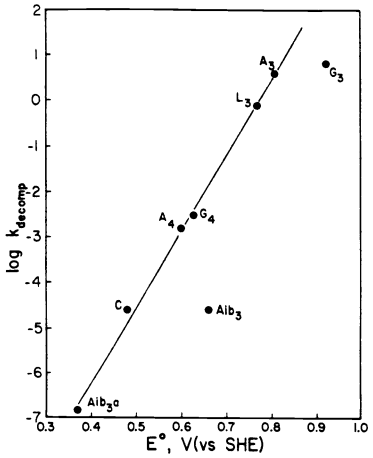

Fig. 6. Rate constants for the redox decomposition of Cu(III) peptides at pH 11 as a function of the electrode potential of the Cu(III,II) peptide couple.

life at pH 11 is two months for $Cu^{III}(H_{-3}Aib_3a)$ compared to 0.1 s for $Cu^{III}(H_{-3}G_3)$. Although G_3 and Aib_3 fall off the correlation line which fits six other Cu(III)-peptides, the trend of stability as a function of E^o is clear. Similar trends are seen at other pH values (Ref. 37).

Photochemical redox decomposition (Ref. 5). All the Cu(III)-peptide complexes are photochemically active and decompose in visible light. The quantum yields for the disappearance of Cu(III) are wavelength dependent as seen for the photolysis of $Cu^{III}(H_{-2}Aib_3)$ in Fig. 7, which also gives the absorption spectrum of this complex. Quantum yields

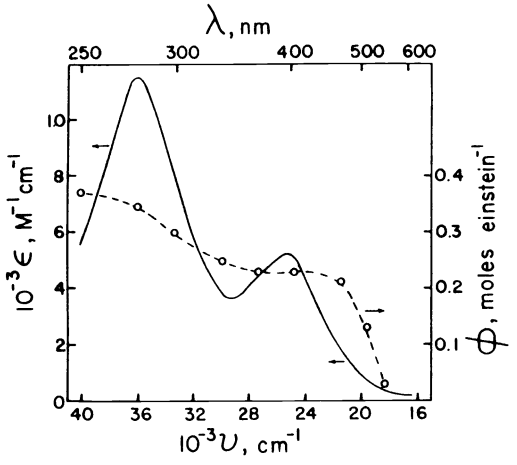

Fig. 7. Absorption spectrum and quantum yield of $Cu^{III}(H_{-2}Aib_3)$.

(moles $einstein^{-1}$) which are 0.34-0.37 at 278-250 nm, drop to 0.21-0.23 at 468-366 nm and decrease to 0.03 at 546 nm. The two Φ plateaus correspond to the two charge transfer absorption bands of the complex. The UV band (278 nm) and the visible band (395 nm) give different redox products as well as different quantum yields. The fall off in Φ above 500 nm is attributed to light absorption by a d-d-transition which is not photoactive.

The photolysis reaction gives Cu(II) and a 50% recovery of the initial Aib_3. The oxidized products are NH_3, acetone, CO_2, Aib_2, Aib, Aiba and Aib_2a as shown in Fig. 8. π-LMCT refers to the visible absorption band, which is assigned to a ligand-to-metal charge transfer from

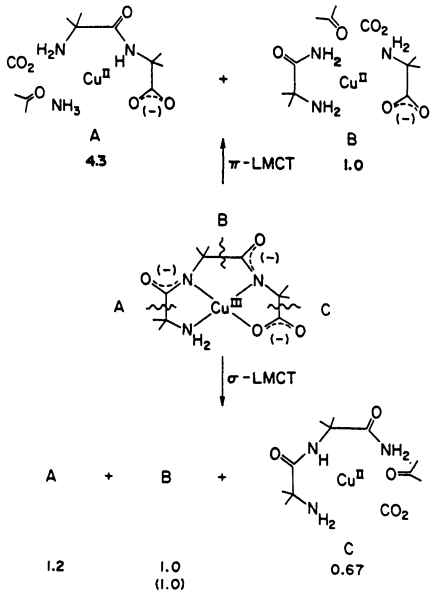

Fig. 8. Oxidized products from the visible (π-LMCT) and UV(σ-LMCT) photodecomposition of $Cu^{III}(H_{-2}Aib_3)$.

the peptide π orbital. σ-LMCT refers to the UV absorption band, which is assigned to a ligand-to-metal charge transfer from the σ coordinate bond. The π-LMCT absorption leads to products A and B in 4.3/1.0 ratio, whereas the σ-LMCT absorption leads to products A, B and C in the ratio 1.2; 1.0; 0.67. The products all result from C-C bond fission with A, B, and C products from the first, second, and third chelate rings, respectively. The initial products are believed to be isocyanates and Schiff bases which hydrolyze to the identified products. In the proposed mechanism the primary photoproducts are σ and π copper(II) amidyl radicals which undergo rapid fragmentation reactions.

The magnitude of the quantum yields is reduced as CH_3 groups on the α-carbon atoms are replaced by hydrogen. Thus, A_3 is less photoactive than Aib_3, and G_4 is much less photoactive than Aib_3G. Methyl groups have the opposite effect on the thermal stability with the interesting result that the Cu(III) peptides which are more stable to thermal redox decomposition are also more sensitive to photochemical decomposition.

Cu(III,II) electron transfer. The kinetics of Cu(III)peptide reactions with reducing agents have been examined for many systems (Ref. 31). The wide range of Cu(III,II) potentials available allow a series of reaction rates to be determined with each reducing agent in order to test the fit to the Marcus theory of electron transfer (Ref. 38).

It is possible to study cross reactions of the type shown in eq 5 because of the spectral

$$Cu^{III}(H_{-2}Aib_3) + Cu^{II}(H_{-3}L) \xrightarrow{k_{12}} Cu^{II}(H_{-2}Aib_3)^- + Cu^{III}(H_{-3}L) \quad (5)$$

shifts which occur in these two types of Cu(III) complexes. The Marcus correlation in eq 6

$$k_{12} = (k_{11}k_{22}K_{12}f)^{1/2} \quad (6)$$

gives the cross exchange rate constant when the two self-exchange rate constants, k_{11} and k_{22}, are known. The self-exchange rate constant for the electron transfer between $Cu^{III}(H_{-2}Aib_3)$ and $Cu^{II}(H_{-2}Aib_3)^-$ has been measured by NMR line broadening of the methyl protons in $Cu^{III}(H_{-2}Aib_3)$ upon the addition of small amounts of $Cu^{II}(H_{-2}Aib_3)^-$ (Ref. 39). Figure 9 shows a plot of log $k_{12}/f^{1/2}$ against log K_{12} where K_{12} is the equilibrium constant for the reaction in eq 5 (Ref. 40). The slope is 0.5 which is predicted by eq 6 provided the k_{22}

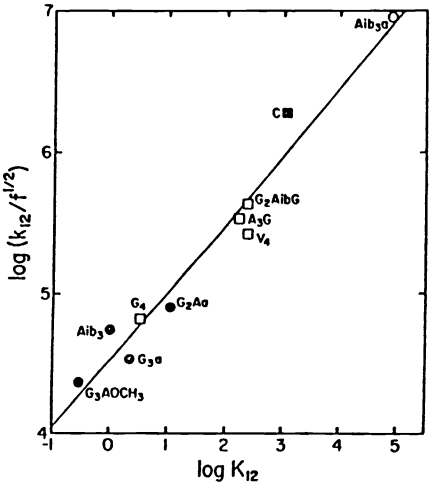

Fig. 9. Marcus plot for the electron transfer reactions of $Cu^{III}(H_{-2}Aib_3)$ with $Cu^{II}(H_{-3}L)$.

values are constant for the eight $Cu^{III,II}(H_{-3}L)$ couples. The average k_{22} value is 2.1 x 10^4 M^{-1} s^{-1} for these complexes. It is noteworthy that the k_{22} values are constant despite the fact that the E^o values vary by 0.43 V. These Cu(III,II) reactions fit the Marcus outer-sphere electron-transfer theory very well.

In order to confirm the outer sphere nature of electron transfer additional cross reactions were measured for reactions with Ru(II) complexes, where there is no possibility for inner-sphere bridging (eq 7 and 8). The self exchange rate constants for the Ru(III,II) electron

$$Cu^{III}(H_{-3}L) + Ru(NH_3)_6^{2+} \longrightarrow Cu^{II}(H_{-3}L) + Ru(NH_3)_6^{3+} \quad (7)$$

$$Cu^{III}(H_{-3}L) + Ru(NH_3)_5py^{2+} \longrightarrow Cu^{II}(H_{-3}L) + Ru(NH_3)_5py^{3+} \quad (8)$$

transfer reactions are known. The rate constants for eq 7 and 8 are accurately predicted by Marcus theory (within a factor of 2) using the self-exchange rate constants measured for the Cu(III,II) peptide couples (Ref. 40).

On the other hand, the reactions between $Ir^{IV,III}Cl_6^{2-}$ and $Cu^{III,II}(H_{-n}L)$ complexes are much faster than predicted. Excellent Marcus plots are obtained, but the apparent self exchange rate constant becomes 3 x 10^8 M^{-1} s^{-1} for $Cu^{III,II}(H_{-n}L)$ (Ref. 41). This increase of four orders of magnitude in the apparent self-exchange rate constant suggests a more facile reaction path exists which involves Cl bridging between Cu and Ir. The axial coordination position is unoccupied in Cu(III) complexes and the axially coordinated water in the Cu(II) complexes is very labile. Hence, the suggested bridging species can form readily, although the association is expected to be very weak.

The reaction kinetics of Cu(III) peptides with $Fe(CN)_6^{4-}$ were measured in order to test the concept of a bridging inner sphere mechanism (Ref. 42). The observed k_{12} rate constants are factors of 4 to 40 greater than the rate constants predicted from the known self exchange rate constants. This corresponds to apparent self exchange rate constants which are 16 to 1600 greater than expected for Cu(III,II). A bridging mechanism is suggested as shown in Fig. 10. In this case ESR spectra of the reaction products show evidence of an associated species: $[Fe^{III}(CN)_6 \cdot Cu^{II}(H_{-2}Aib_3)]^{4-}$.

In conclusion, two reaction paths for electron transfer reactions of Cu(III,II) peptides are proposed. Outer-sphere electron transfer is rapid, with rate constants of (2.0 to 5.5) x 10^4 M^{-1} s^{-1}, despite the change of coordination number of copper from 4 to 6 and the

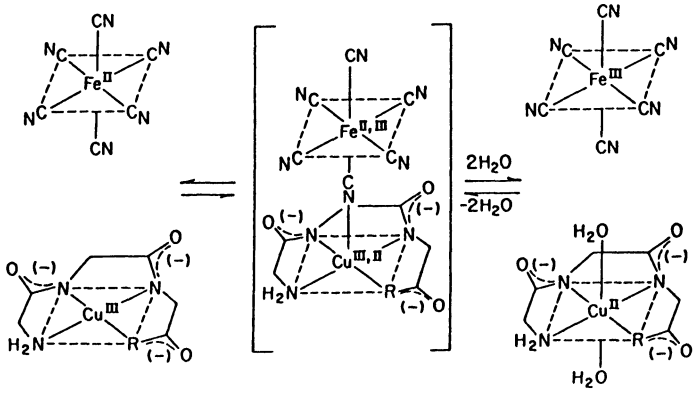

Fig. 10. Proposed inner-sphere mechanism for $Cu^{III}(H_{-3}L)$ and $Fe^{II}(CN)_6^{4-}$.

significant changes in equatorial copper bond distances for Cu(III) and Cu(II). In addition, an enhanced reaction path with inner-sphere electron transfer is suggested. In these inner sphere reactions the bridging group is not transferred, however, the bridging group enhances the electron transfer.

NICKEL(III) PEPTIDES

Properties of nickel(III) peptide complexes. The evidence for trivalent nickel includes chemical and electrochemical oxidation, redox stoichiometry, sluggish substitution reactions, and UV-visible spectral shifts. In addition, electron spin resonance indicates that Ni(III) is present and gives information about its coordination geometry in the frozen solution state (Ref. 43). The ESR spectra of Ni(III) complexes obtained from freezing aqueous solutions correspond to an unpaired electron in the d_{z^2} orbital in a tetragonally distorted (axial elongation) octahedral geometry. The $g_{\perp}$ values are larger than the $g_{||}$ values indicating that the complexes have axially coordinated water. When the solutions contain varying amounts of ammonia the frozen spectra show that one or two NH_3 molecules replace the axial H_2O. The $g_{||}$ band splits into a triplet with one coordinated NH_3 and becomes a quintet with two coordinated NH_3 molecules. As five and six nitrogens are coordinated to the nickel the $g_{\perp}$ and $g_{||}$ values move closer together because the degree of tetragonal distortion is less.

It is much easier to find axially coordinated ligands in the frozen state than is the case for the same composition of solutions at room temperature. Although the solutions are plunged into liquid nitrogen for a relatively quick freeze, the process shifts the equilibrium by many orders of magnitude to give axial species in the frozen state which may be in negligible concentration at room temperature.

Cyclic voltammetry of Ni(II)-peptides in the presence of coordinating ligands is an effective method for the determination of Ni(III)-peptide association constants (Ref. 44). The ligands do not coordinate to the Ni(II) peptides, but shift the potential of the Ni(III,II) couple because of ligand coordination to Ni(III). Stability constants at 25°C vary from 1100 to 50 M^{-1} (in the order: imidazole > NH_3 ≃ N_3^- > pyridine) but are relatively independent of the nature of the peptide. For the $Ni^{III}(H_{-3}G_3a)NH_3$ complex the association constant is 270 M^{-1} at 25.0°C, ΔH^o is -3.6 ± 0.4 kcal mol^{-1} and ΔS^o is 1.0 ± 1.2 cal deg^{-1} mol^{-1}. The second ammonia adduct cannot be detected at room temperature.

Chelating ligands with nitrogen donors form strong adducts with Ni(III) peptides. The addition of terpyridyl to $Ni^{III}(H_{-2}GAG)$ gives a frozen ESR spectra that indicates terpy coordinates to both axial positions (Fig. 11). Shifts in the room temperature ESR permit a stability constant ($\log K_1$ = 11.8) to be determined for the 1:1 adduct (Ref. 45). This is a very stable complex.

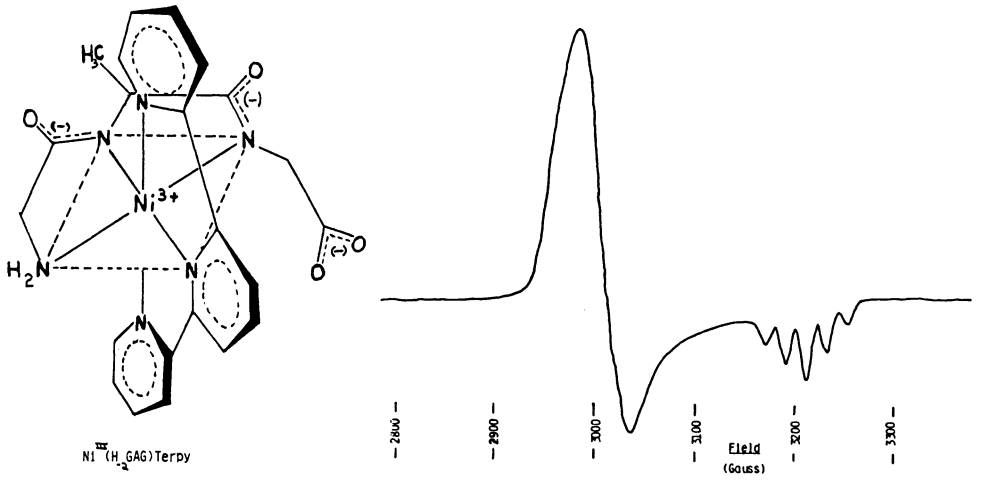

Fig. 11. Proposed structure and ESR spectrum (-150°C) for $Ni^{III}(H_{-2}GAG)$terpy.

Bis(peptide) complexes of Ni(III) form in the presence of excess peptide as illustrated in Fig. 12 for G_3. The frozen ESR as well as room temperature ESR and UV-VIS spectra show

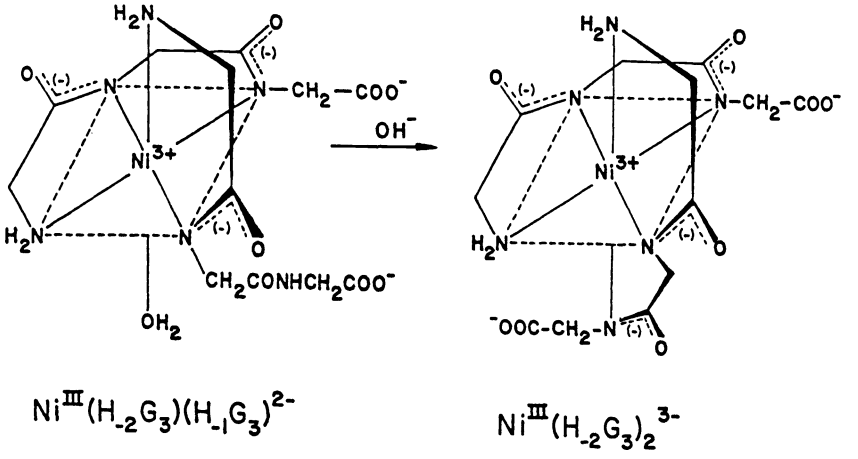

Fig. 12. Proposed structures for bis(triglycine) complexes of Ni(III).

large shifts corresponding to the bidentate addition of the second G_3 to give $Ni^{III}(H_{-2}G_3)\cdot(H_{-1}G_3)^{2-}$. This species converts to a tridentate adduct $Ni^{III}(H_{-2}G_3)_2^{3-}$ with a pK_a value of 11 (Ref. 46).

The ternary and bis peptide complexes of Ni(III) are slower to undergo thermal redox decomposition than the 1:1 complexes. The E^0 values for the various 1:1 Ni(III,II) peptide complexes fall in a narrower range (0.79 to 0.96 V) (Ref. 27) than is the case for the corresponding Cu(III,II) potentials. On the other hand, adduct formation with Ni(III) is very important and will greatly shift E^0 to lower values.

The $Ni^{III}(H_{-2}Aib_3)$ complex is also photoactive with quantum yields only slightly less than the $Cu^{III}(H_{-2}Aib_3)$ complex (Ref. 5). However, the absorption bands are at lower wavelength (263 nm and 352 nm) so the complex is less subject to decomposition by visible radiation.

Axial substitution reactions of Ni(III) peptides are extremely rapid with rate constants too large to measure by stopped-flow methods. The exchange rate constant for axial water is greater than 4×10^6 s^{-1} (Ref. 44). Equatorial substitution reactions of Ni(III) are sluggish with the exception of the terminal N(peptide) or N(amide) groups. When $Ni^{III}(H_{-3}G_4a)$ is mixed with acid, rapid outside protonation ($K = 2.2$ M^{-1}) gives $Ni^{III}(H_{-3}G_4a)H^+$, which undergoes substitution of the terminal peptide group with a rate constant of 15.3 s^{-1} to form $Ni^{III}(H_{-2}G_4a)$ (Ref. 48). Subsequent substitution reactions are not observed. The redox decomposition reactions in acid limit the measurements, but substitution rate constants of the other equatorial positions are not larger than 10^{-3} s^{-1}.

Electron transfer Ni(III,II). Twenty-five cross reactions between Ni(III) peptides and Ni(II) peptides have been used to evaluate their self exchange rate constants (Ref. 44). Unlike the Cu(III,II) peptides, the Ni(III,II) peptides show a large variation in the magnitude of k_{11} with the structure of the peptide complex. These k_{11} values can be classified into the following groups: triply-deprotonated peptides (1.2×10^5 M^{-1} s^{-1}); doubly-deprotonated peptides (1.3×10^4 M^{-1} s^{-1}) except for the complexes of Aib_3 and $AAib_2$ (5.5×10^2 M^{-1} s^{-1}). The cross reactions are catalyzed by bridging ligands with a 10-fold increase in the rate constant in the presence of 5×10^{-3} M Br^-. The order of enhanced reactivity from bridging ligands is $Br^- > Cl^- > N_3^-$ and there is no enhancement with F^-.

The reasons for the large variation in k_{11} values for the different nickel peptide complexes is not clear, but some enhancement may be due to association between the complexes. The $Ni^{III}(H_{-2}Aib_3)$ complex gives rate constants which are consistent for outer-sphere electron transfer with several different reducing agents. Table 1 compares the observed and

TABLE 1. Electron transfer rate constants for $Ni^{III,II}(H_{-2}Aib_3)^{0,-}$

Reaction	k_{12}, M^{-1} s^{-1} obsd	predicted*
$Ni^{III}(H_{-2}Aib_3)$ + $Ni^{II}(H_{-2}Aib_3)^-$, ^1H nmr	< 800	550*
+ $Cu^{II}(H_{-2}Aib_3)^-$	8.1×10^4	10.7×10^4
+ $Co^{II}(Me_6[14]dieneN_4)^{2+}$	135	77
+ $Co^{II}(Me_2pyro[14]trieneN_4)^{2+}$	2.5×10^3	3.1×10^3
$Ir^{IV}Cl_6^{2-}$ + $Ni^{II}(H_{-2}Aib_3)^-$	5.8×10^7	3.5×10^4

*Predictions use $k_{11} = 550$ M^{-1} s^{-1} based on many $Ni^{III,II}(H_{-2}Aib_3)$ cross reactions with $Ni^{III,II}(H_{-n}L)$.

predicted k_{12} values based on a k_{11} value of 550 M^{-1} s^{-1} for $Ni^{III,II}(H_{-2}Aib_3)^{0,-}$. The ^1H NMR line broadening technique gave only an upper limit because the electron transfer was so slow. There is excellent agreement for the cross reaction rate constants of $Ni^{III}(H_{-2}Aib_3)$ with $Cu^{II}(H_{-2}Aib_3)^-$ (Ref. 49) and the two macrocyclic[14]N_4 complexes of Co(II) (Ref. 50). These results suggest that a value of 550 M^{-1} s^{-1} represents a valid outer-sphere electron-transfer rate constant for this nickel complex. Table 1 also shows that the k_{12} rate constant for the reaction of $Ni^{II}(H_{-2}Aib_3)^-$ with $IrCl_6^{2-}$ is a factor of 1.7×10^3 larger than expected for this k_{11} value. Hence, an inner-sphere electron transfer path again appears to be important. In the case of Ni(III,II) peptides the enhancement due to the inner-sphere path even more pronounced than is the case with Cu(III,II) peptides.

Acknowledgment - These investigations were supported by Public Health Service Grants GM-12152 and GM-19775 from the National Institute of General Medical Sciences.

REFERENCES

1. D.W. Margerum and G.R. Dukes, Metal Ions in Biological Systems, Vol. 1, p. 157-212, Marcel Dekker, New York (1974).
2. J.S. Rybka and D.W. Margerum, Inorg. Chem. 19, 2784-2790 (1980).
3. F.P. Bossu, K.L. Chellappa and D.W. Margerum, J. Am. Chem. Soc. 99, 2195-2203 (1977).
4. R.M. Smith and A.E. Martell, Ed., Critical Stability Constants, Vol. 1, Plenum Press, New York (1974).
5. A.W. Hamburg and D.W. Margerum, to be published.
6. H.C. Freeman, Adv. Protein Chem. 22, 257-424 (1967).
7. C.E. Bannister, D.W. Margerum, J.M.T. Raycheba and L.F. Wong, Faraday Symposia, The Chemical Society, No. 10, p. 78 (1975).
8. C.E. Bannister, J.M.T. Raycheba and D.W. Margerum, Inorg. Chem. 21, 1106-1112 (1982).
9. M.T. Barnet, H.C. Freeman, D.A. Buckingham, I.N. Hsu and D. Van der Helm, Chem. Commun. 367 (1970).
10. E.B. Paniago and D.W. Margerum, J. Am. Chem. Soc. 94, 6704-6710 (1972).
11. L.F. Wong, J.C. Cooper and D.W. Margerum, J. Am. Chem. Soc. 98, 7268-7274 (1976).
12. J.C. Cooper, L.F. Wong and D.W. Margerum, Inorg. Chem. 17, 261-266 (1978).
13. J.S. Rybka, J.L. Kurtz, T.A. Neubecker and D.W. Margerum, Inorg. Chem. 19, 2791-2796 (1980).
14. J.S. Rybka and D.W. Margerum, Inorg. Chem. 20, 1453-1458 (1981).
15. M.P. Youngblood and D. W. Margerum, Inorg. Chem. 19, 3072-3077 (1980).
16. M.P. Youngblood, K.L. Chellappa, C.E. Bannister and D.W. Margerum, Inorg. Chem. 20, 1742-1747 (1981).
17. Y.H.C. Wang and D.W. Margerum, to be published.
18. C.E. Bannister and D.W. Margerum, Inorg. Chem. 20, 3149-3155 (1981).
19. M.M. Kreevoy and D.E. Konasewich, Adv. Chem. Phys. 21, 243 (1972).
20. A.I. Hassid, M.M. Kreevoy and T.M. Liang, Symp. Faraday Soc., No. 10, p. 69 (1975).
21. A.O. Cohen and R.A. Marcus, J. Phys. Chem. 72, 4249 (1968).
22. R.A. Marcus, J. Phys. Chem. 72, 891 (1968).
23. D.W. Margerum, ACS Adv. in Chem., Symp. Series 198 (1982).
24. G.K. Pagenkopf and D.W. Margerum, J. Am. Chem. Soc. 92, 2683-2686 (1970).
25. B. Schwerderski, J.M.T. Raycheba and D.W. Margerum, to be published.
26. J.C. Cooper, L.F. Wong, D.L. Venezky and D.W. Margerum, J. Am. Chem. Soc. 96, 7560-7562 (1974).
27. E.B. Paniago, D.C. Weatherburn and D.W. Margerum, Chem. Commun., 1427-1428 (1971).
28. G.L. Burce, E.B. Paniago and D.W. Margerum, Chem. Commun., 261-262 (1975).
29. F.P. Bossu, E.B. Paniago, D.W. Margerum, S.T. Kirksey, Jr. and J.L. Kurtz, Inorg. Chem. 17, 1034-1042 (1978).
30. J.L. Kurtz, G.L. Burce and D.W. Margerum, Inorg. Chem. 17, 2454-2460 (1978).
31. D.W. Margerum and G.D. Owens, Metal Ions in Bioligical Systems, Vol. 12, p. 75-132, Marcel Dekker, New York (1981).
32. D.W. Margerum, K.L. Chellappa, F.P. Bossu and G.L. Burce, J. Am. Chem. Soc. 97, 6894-6896 (1975).
33. M.P. Youngblood and D.W. Margerum, Inorg. Chem. 19, 3072-3077 (1980).
34. L.L. Diaddario, W.R. Robinson and D.W. Margerum, to be published.
35. J.P. Hinton and D.W. Margerum, to be published.
36. T.A. Neubecker, S.T. Kirksey, Jr., K.L. Chellappa and D.W. Margerum, Inorg. Chem. 18, 444-448 (1979).
37. L.L. Diaddario, R.A. Read, J.P. Hinton and D.W. Margerum, to be published.
38. R.A. Marcus, J. Phys. Chem. 67, 853 (1963); J. Chem. Phys. 43, 679 (1965).
39. C.A. Koval and D.W. Margerum, Inorg. Chem. 20, 2311-2318 (1981).
40. J.M. Anast, A.W. Hamburg and D.W. Margerum, to be published.
41. G.D. Owens and D.W. Margerum, Inorg. Chem. 20, 1446-1453 (1981).
42. J.M. Anast and D.W. Margerum, Inorg. Chem. 21, 0000 (1982).
43. A.G. Lappin, C.K. Murray and D.W. Margerum, Inorg. Chem. 17, 1630-1634 (1978).
44. C.K. Murray and D.W. Margerum, Inorg. Chem. 21, 0000 (1982).
45. T.L. Pappenhagen and D.W. Margerum, to be published.
46. G.E. Kirvan and D.W. Margerum, to be published.
47. F.P. Bossu and D.W. Margerum, Inorg. Chem. 16, 1210-1214 (1977).
48. E.J. Subak, Jr., V.M. Loyola and D.W. Margerum, to be published.
49. G.D. Owens, D.A. Phillips, J.J. Czarnecki, J.M.T. Raycheba and D.W. Margerum, to be published.
50. K. Kumar and D.W. Margerum, to be published.